FEBS Letters 584 (2010) 3533–3539

journal homepage: www.FEBSLetters.org

Crystal structure of tubulin folding cofactor A from *Arabidopsis thaliana* and its β-tubulin binding characterization

Lu Lu [a,b], Jie Nan [a], Wei Mi [a], Lan-Fen Li [a], Chun-Hong Wei [a,b], Xiao-Dong Su [a,c,*], Yi Li [a,b,**]

[a] *The National Laboratory of Protein Engineering and Plant Genetic Engineering, College of Life Sciences, Peking University, Beijing 100871, China*
[b] *Peking-Yale Joint Center for Plant Molecular Genetics and Agrobiotechnology, Beijing 100871, China*
[c] *Laboratory of Chemical Genomics, Shenzhen Graduate School of Peking university, Shenzhen 513055, China*

ARTICLE INFO

Article history:
Received 17 May 2010
Revised 5 July 2010
Accepted 12 July 2010
Available online 16 July 2010

Edited by Christian Griesinger

Keywords:
Tubulin folding cofactor A (TFC A)
β-Tubulin binding
Crystal structure
Arabidopsis

ABSTRACT

Microtubules are composed of polymerized α/β-tubulin heterodimers. Biogenesis of assembly-competent tubulin dimers is a complex multistep process that requires sequential actions of distinct molecular chaperones and cofactors. Tubulin folding cofactor A (TFCA), which captures β-tubulin during the folding pathway, has been identified in many organisms. Here, we report the crystal structure of *Arabidopsis thaliana* TFC A (KIESEL, KIS), which forms a monomeric three-helix bundle. The functional binding analysis demonstrated that KIS interacts with β-tubulin in plant. Furthermore, mutagenesis studies indicated that the α-helical regions of KIS participate in β-tubulin binding. Unlike the budding yeast TFC A, the two loop regions of KIS are not required for this interaction suggesting a distinct binding mechanism of TFC A to β-tubulin in plants.

Structured summary:
MINT-7968902, MINT-7968915, MINT-7968951, MINT-7968966: *KIS* (uniprotkb:O04350) *physically interacts* (MI:0915) with *Tub9* (uniprotkb:P29517) by *anti tag coimmunoprecipitation* (MI:0007)
MINT-7968928: *KIS* (uniprotkb:O04350) and *Tub9* (uniprotkb:P29517) *physically interact* (MI:0915) by *bimolecular fluorescence complementation* (MI:0809)

1. Introduction

Microtubules are polymers of α/β-tubulin heterodimers with complex dynamic structures and multiple protein-interacting surfaces [1]. Cellular synthesis of tubulin heterodimers is a multistep process involving several molecular chaperones and tubulin folding cofactors (TFCs) [2]. Newly synthesized α- and β-tubulin polypeptides are first associated with prefoldin [3], which then transfers them to the cytosolic chaperonin CCT (Chaperonin Containing-TCP1) to form a tubulin–CCT complex [4]. Next, five TFCs, termed TFC A–E, facilitate the subsequent tubulin folding pathway [5–7]. TFC A and TFC B bind to β-tubulin and α-tubulin, respectively, which then deliver β-tubulin to TFC D and α-tubulin to TFC E separately. After that, protein complexes resulting from the two pathways converge to form a multimeric supercomplex containing TFC D, TFC E, α- and β-tubulin. Binding of TFC C to this supercomplex stimulates GTP hydrolysis by the bound β-tubulin and the release of the α/β-tubulin heterodimers [8]. A small G-protein Arl2 has been reported to regulate the pathway by sequestering the TFC D [9].

TFC A was first purified from bovine testis [10,11] and was recognized as a molecular chaperone involved in β-tubulin folding [11]. Mammalian TFC A (CoA) can release β-tubulin from the intermediate complex C_{300} and then bind non-covalently to β-tubulin [10]. Though not required for β-tubulin folding in vitro [6], TFC A serves as a reservoir of excess β-tubulin [2,12]. Down-regulation of *TFC A* expression in Hela cell results in the destruction of the microtubule cytoskeleton and cell death [13]. Rbl2p, the TFC A ortholog in *Saccharomyces cerevisiae*, functions to protect cells from lethal β-tubulin overexpression by binding transiently to the free β-tubulin until it forms a non-toxic aggregate [14,15].

Two distinct models of interaction between the TFC A and β-tubulin have been proposed based on the structural studies of the TFC A proteins from yeast and mammalian [16,17]. Rbl2p has

Abbreviations: TFC, tubulin folding cofactor; CoA, cofactor A; KIS, KIESEL; PIPES, piperazine-*N*,*N*′-bis (2-ethanesulfonic acid); EGTA, ethylene glycol bis (2-aminoethyl ether)-*N*,*N*,*N*′,*N*′-tetraacetic acid; RMSD, root mean square deviations

* Corresponding author at: The National Laboratory of Protein Engineering and Plant Genetic Engineering, College of Life Sciences, Peking University, Beijing 100871, China. Fax: +86 10 62765669.
** Corresponding author at: The National Laboratory of Protein Engineering and Plant Genetic Engineering, College of Life Sciences, Peking University, Beijing 100871, China. Fax: +86 10 62756903.
E-mail addresses: xdsu@pku.edu.cn (X.-D. Su), liyi@pku.edu.cn (Y. Li).

0014-5793/$36.00
doi:10.1016/j.febslet.2010.07.017

been shown to crystallize into antiparallel α-helical homodimer and a four-helix bundle is formed with two long helices from each monomer packing together [16]. Computational docking and mutagenesis assays illustrated that dimerization is important for the interaction between Rbl2p and β-tubulin, and the loop regions of the homodimer mediate the β-tubulin binding [18]. However, human CoA crystallizes as a monomer and the α-helical regions, but not the linker loops, are supposed to be involved in binding to β-tubulin by the peptide mapping analysis [17].

Arabidopsis TFC A is encoded by the *KIESEL (KIS)* gene, the mutations of which lead to cell morphogenesis defects and impaired cell division phenotypes [19,20]. *KIS* has been shown to play an important role in the control of the ratio between α- and β-tubulin monomers in plant cell [20]. Moreover, KIS is predicted to interact with the prefoldin complex participating in the early steps of microtubule biogenesis [21]. In spite of the genetic studies, the biochemical and structural information of KIS are largely unknown. To understand the recognition mechanism of tubulin in plants, we have now determined the crystal structure of KIS at 1.6-Å resolution and revealed that KIS interacts with β-tubulin in plants. The site-specific mutagenesis showed that the α-helical regions are responsible for β-tubulin binding, whereas the two loop regions connecting the three helices are not involved in this interaction, differing greatly from that of Rbl2p. These studies provide insights into the TFC A/β-tubulin interactions in plants.

2. Materials and methods

2.1. Protein preparation, crystallization and data collection

The preparation, crystallization of the KIS protein and details of X-ray diffraction data collection of the crystal were described previously [22].

2.2. Structure determination and refinement

The structure of KIS was solved by molecular replacement using the program MolRep in the CCP4 package [23]. The Rbl2p structure (PDB ID: 1QSD [16]) was used as the search model. Refinement was carried out with the program Phenix [24] combined with manual adjustment using software COOT [25]. The stereochemistry quality of the structure was checked by PROCHECK [26]. The refinement statistics of the structure are listed in Table 1. The coordinates and experimental structural factors have been deposited in the Protein Data Bank with accession number 3MXZ.

Table 1
Summary of refinement statistics.

	KIS
Space group	$I4_1$
Unit cell parameters (Å)	$a = b = 54.97$, $c = 67.42$
Resolution (Å)	17.68–1.60
R_{factor} (%)	17.6
R_{free}[a] (%)	20.8
No. protein atoms	813
No. nitrate ions	2
No. water molecules	188
Average B-factor (Å^2)	23.15
R.M.S.D. bond lengths (Å)	0.007
R.M.S.D. bond angles (°)	1.064
Ramachandran plot statistics (%)	
Most favored region	100

[a] 4.93% of the total reflections were set aside for R_{free} calculation.

2.3. Plasmid construction

KIS and *Arabidopsis* β-tubulin 9 (*TUB9*) were amplified by PCR from the cDNA library of *Arabidopsis thaliana*. HA and FLAG epitope tags were added to *KIS* or *TUB9* using gene specific primers for PCR. Restriction fragments were first ligated into a cauliflower mosaic virus 35S-based pRTL2 vector [27]. Then the fragments were cleaved from *pRTL2-HA-KIS* or *pRTL2-FLAG-TUB9* with *Pst*I and inserted into the *Pst*I site of the vector pCAMBIA1301. For constructs used in BiFC experiments, *KIS* and *TUB9* were PCR amplified and cloned into the pSPYCE-35S and pSPYNE-35S vectors, respectively [28].

Site-directed mutagenesis was introduced into *KIS* gene by the overlap extension PCR method. All the DNA constructs were confirmed by DNA sequencing and used in transient expression system for coimmunoprecipitation or in the *Escherichia coli* expression system for protein production.

2.4. Coimmunoprecipitation assays

The *Agrobacterium* infiltration was carried out according to the method previously described [29]. *Agrobacterium tumefaciens* carrying constructs of 35S-*KIS-HA* or the mutants of *KIS* and 35S-*FLAG-TUB9* were mixed at a ratio of 1:1 for co-infiltration. Total proteins were extracted from *N. benthamiana* leaves with IP buffer (50 mM PIPES pH 6.9, 1 mM $MgCl_2$, 1 mM EGTA, 5 mM dithiothreitol, 0.1% NonidetP-40, and 1× Complete Protease Inhibitor cocktail (Roche)) 72 h after infiltration. About 1 mg of soluble protein was incubated with 0.5 μg anti-FLAG monoclonal antibody (Sigma) or 0.5 μg anti-HA monoclonal antibody (Tiangen, Beijing) at 4 °C for 1 h, followed by an addition of 30 μl of protein G Sepharose-4 fast flow beads (GE) and incubation for another 3 h. Then the beads were washed four times with IP buffer. After washing, the beads were resuspended in SDS–PAGE loading buffer and subjected to immunoblot analysis. The immunocomplex was detected with anti-HA monoclonal (Roche) or anti-FLAG monoclonal (Sigma) antibodies.

2.5. Bimolecular fluorescence complementation (BiFC) assays

Epidermal cells of tobacco leaves were co-infiltrated with *Agrobacterium* strains containing the BiFC constructs. Complementation of YFP was visualized under a confocal microscope.

2.6. Circular dichroism (CD) spectroscopy assays

All CD spectra of proteins were measured in a J-715 CD spectropolarimeter (JASCO, Japan) at 298 K by adding 400 μl (0.1 mg/ml) protein sample to a 2-mm quartz cuvette. Wavelength scans were performed between 190 and 250 nm with a 2-nm bandwidth and a 0.5-nm step size at a rate of 1 nm/s. Each spectrum represents an average of three scans.

2.7. Size-exclusion chromatography (SEC) assays

The protein extracts were prepared in 50 mM Tris–HCl, pH 7.5, 150 mM NaCl, 0.1% NonidetP-40, and 1× Complete Protease Inhibitor cocktail (Roche). Approximately 400 μg of soluble protein was applied to a Superdex 200 10/300 GL column (GE healthcare). The column was eluted with the extraction buffer and fractions (0.5 ml each) were collected and subjected to immunoblot analysis with anti-HA monoclonal antibody. The protein standards were as follows: ferritin (440 kDa), aldolase (158 kDa), conalbumin (75 kDa), ovalbumin (43 kDa), carbonic anhydrase (29 kDa), ribonuclease A (13.7 kDa).

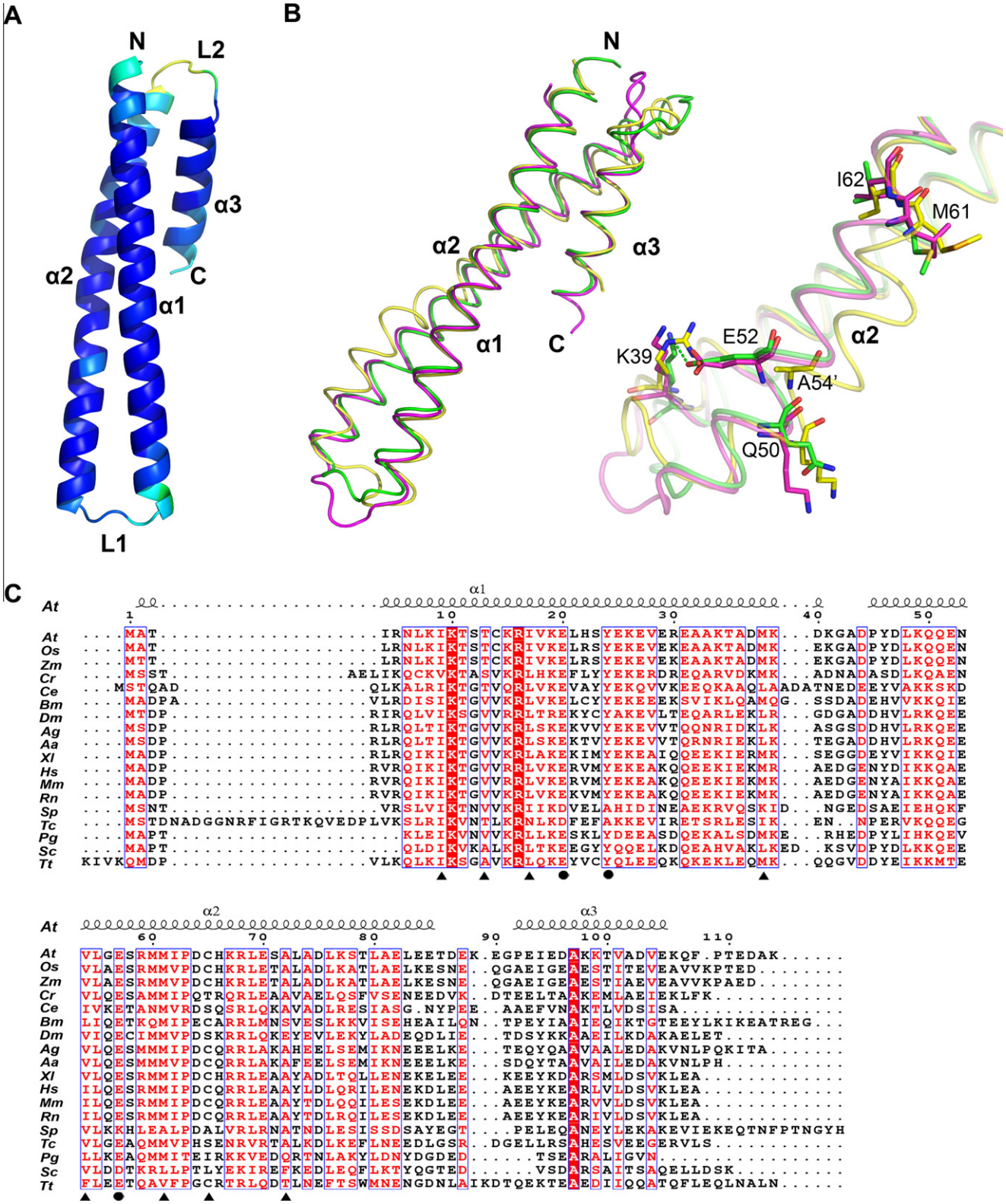

Fig. 1. (A) The overall structure of KIS in ribbon colored according to the B-factor value, from blue to yellow in the order of increasing B-factor. (B) Structure superimposition of human CoA (yellow), Rbl2p (magenta) and KIS (green). A zoom-in view of the N-terminal half of the α2 helix is displayed on the right. The residues of KIS are labeled and residue of human CoA (A54′) is labeled by prime marks on the residue number. The dashed lines indicate salt bridge. (C) Secondary structure-based multiple sequence alignment of TFC A from different organisms was generated with CLUSTALW [35] and drawn with ESPript [36]. Identical residues are highlighted in red and the conserved residues are shown in red letters. Critical residues of KIS involved in β-tubulin binding are marked by black dots. Residues located at the Rbl2p dimer interface are marked by triangles. Short names are used for organisms: At, *Arabidopsis thaliana*; Os, *Oryza sativa*; Zm, *Zea maize*; Cr, *Chlamydomonas reinhardtii*; Ce, *Caenorhabditis elegans*; Bm, *Brugia malayi*; Dm, *Drosophila melanogaster*; Ag, *Anopheles gambiae*; Aa, *Aedes aegypti*; Xl, *Xenopus laevis*; Hs, *Homo sapiens*; Mm, *Mus musculus*; Rn, *Rattus norvegicus*; Sp, *Schizosaccharomyces pombe*; Tc, *Trypanosoma cruzi*; Pg, *Pichia guilliermondii*; Sc, *Saccharomyces cerevisiae*; Tt, *Tetrahymena thermophila*.

3. Results

3.1. Overall structure of KIS

The crystal structure of KIS has been solved and refined to 1.6 Å. The last six residues are not built and some residues in the loop regions are not well defined.

KIS forms a monomer in the crystal lattice and also in solution as results from gel filtration assays (data not shown). The whole molecule has an elongated shape with a length of 64 Å and a width of about 14 Å. The overall structure of KIS is similar to those of Rbl2p monomer (PDB ID: 1QSD [16]) and human CoA (PDB ID: 1H7C [17]), consisting of three α-helices connected by two linker loops. The two long helices (α1 and α2) and one short helix (α3) pack together into an antiparallel bundle (Fig. 1A). The α1 helix spans residues 1–41, the α2 helix spans residues 45–85, and the α3 helix spans residues 92–105. The loop2 (L2) connecting the α2- and α3-helices shows a poor electron density, suggesting that this loop is flexible in the free form of KIS.

Pro63 is the residue in the helix that exhibits a low helix propensity and it induces a bend of about 10° in the helical axis of the α2 helix, resulting in a slightly convex surface formation. The presence of a proline residue at this position is a highly conserved character in the TFC A family (Fig. 1C).

3.2. Structure comparison

Sequence comparison of TFC A from different organisms showed that KIS shares about 31% identity with Rbl2p and 45% identity with human CoA. KIS and Rbl2p monomer have three helices that are with a root mean square deviation (RMSD) of 1.6 Å for 85 Cα atoms. Most of the helical regions coincide well (Fig. 1B). Though KIS and human CoA show higher sequence identity, the RMSD for KIS and human CoA is 2.1 Å for 75 Cα atoms. The α-helices of KIS and human CoA are almost superimposable except for the N-terminal half of the α2 helix. The α2 helix of KIS does not have so extensive helix distortion as human CoA, with Cα deviations of up to 5 Å between the two proteins. The deviation region of the N-terminal part of α2 helix consists of residues Gln50-Ile62. The residue Glu52 of KIS projects the side chain toward Lys39 in the α1 helix to form a potential salt bridge (Fig. 1B). This salt bridge has also been observed between Glu52 and Lys38 in Rbl2p, but is lost in human CoA between the corresponding residues Ala54 and Arg41. This may partially contribute to the shifts of the α2 helix. The largest difference in the backbone φ angle between these two proteins locates at Ser58 with −56° in KIS, comparing with −107° for the corresponding residue Ser60 in human CoA. Furthermore, the loop regions are different among the three proteins (Fig. 1B). The loop1 (L1) connecting the α1- and α2-helices shows different orientations in each protein. In addition, the 3_{10} helix in the L2 loop of human CoA is not present in KIS or in Rbl2p.

Though these three proteins have similar topology, the aggregation states of them are different. Rbl2p has been reported as a homodimer in crystal. The α1- and α2-helices of one monomer run antiparallel to the corresponding helices of the other monomer to form a four-helix bundle [16]. In the structure of KIS, only an artificial dimer due to crystal packing is observed and it is different from the dimer of Rbl2p (data not shown). This suggests that KIS exists mainly as monomer, similar to the report on human CoA [17].

3.3. Interactions between KIS and β-tubulin

TFC A is a chaperone in the β-tubulin folding pathway; both Rbl2p and human CoA can interact with β-tubulin [14,30]. To determine whether KIS can interact with β-tubulin in planta, we first performed coimmunoprecipitation assay by coexpressing KIS-HA and FLAG-TUB9 in transient expression system in *N. benthamiana*. The recombinant protein was immunoprecipitated with anti-HA and anti-FLAG antibodies, respectively. As shown in Fig. 2A, KIS-HA was present in the FLAG-TUB9 immune complex. The reciprocal immunoprecipitation experiments also detected the interaction between β-tubulin and KIS. Bimolecular fluorescence complementation (BiFC) analysis was carried out to further confirm the interaction in vivo. The C-terminal half of YFP (c-YFP) was fused to KIS and the N-terminal half of YFP (n-YFP) was fused to TUB9. Then the two constructs were delivered into the leaf cells of *N. benthamiana*. As seen in Fig. 2B, strong fluorescence was observed in the leaf epidermal cells of tobacco coexpressing the KIS-cYFP and TUB9-nYFP, whereas only marginal fluorescence was detected in the negative control cells. Taken together, our data support the hypothesis that KIS interacts with β-tubulin in the plant cell.

3.4. Mutation analysis of the residues of KIS responsible for β-tubulin binding

It has been proposed that Rbl2p binds to β-tubulin as a dimer. The N-terminus residues Pro3 and Thr4, the residues in the L1 loop connecting α1- and α2-helices of one monomer, and the residues in the L2 loop connecting α2- and α3-helices of the other monomer are supposed to mediate the interaction with β-tubulin [18]. However, human CoA has been shown to interact with β-tubulin via the residues in three α-helices [17]. Then, site-directed mutagenesis of KIS was made to determine the contributions of some residues to β-tubulin binding. The targets for mutagenesis analyses are residues have been reported to be the potential β-tubulin binding sites in Rbl2p or in human CoA. In addition, some conserved residues are selected in our mutation studies. To reduce the number of alleles,

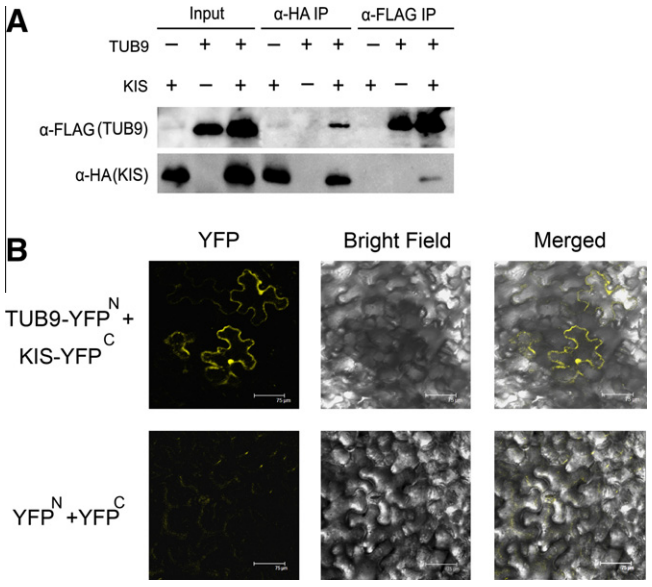

Fig. 2. Interaction of KIS with β-tubulin in vivo. (A) Coimmunoprecipitation assays. The total proteins were extracted from *N. benthamiana* leaves expressing KIS-HA and FLAG-TUB9, and were immunoprecipitated with anti-HA or anti-FLAG antibodies. The immune complex was detected by immunoblotting with anti-FLAG or anti-HA antibodies. The input indicated the total soluble extracts. (B) Bimolecular fluorescence complementation (BiFC) analysis of in vivo interaction between KIS and TUB9. The epidermal leaves of the *N. benthamiana* expressing TUB9-nYFP and KIS-cYFP or the nYFP and cYFP were visualized under a confocal microscope. The results shown are representative of three independent experiments.

we created some mutations that two or more adjacent residues were mutated to alanines.

The binding of β-tubulin for each mutant was tested using coimmunoprecipitation experiments. As shown in Fig. 3, the interaction of mutants E20A, Y24A and E57A with β-tubulin significantly dropped. CD spectra assay were performed to rule out the possibility of incorrect protein folding (Fig. 4A). Glu20 and Tyr24 are located in the middle part of the α1 helix and the corresponding residues in Rbl2p have been reported to be the Rbl2p homodimer interface. To see if the decrease of β-tubulin binding is due to changes of oligomerization, aggregation states of these mutants in vivo in plants were analyzed. Protein extracts from *N. benthamiana* leaves overexpressing the wild-type of KIS or the other mutants were fractionated by SEC and the products of the column fractions were monitored by immunoblotting using anti-HA antibodies. The extracts of untreated plants were analyzed as a control. As shown in Fig. 4B, both the wild-type and the mutants of KIS proteins from plants showed similar column distributions (fractions 18–24), suggesting that these mutation did not affect the oligomeric state of KIS protein in vivo and these two residues might directly participate in β-tubulin recognition. To further understand their roles in β-tubulin binding, mutants of E20Q and Y24F were constructed and analyzed using same methods as described above. In contrast to the significant drop of β-tubulin recognition with ala mutants, both mutations of E20Q and Y24F had slight effects on the interaction, suggesting that a polar and a big hydrophobic group are needed for Glu20 and Tyr24 positions, respectively.

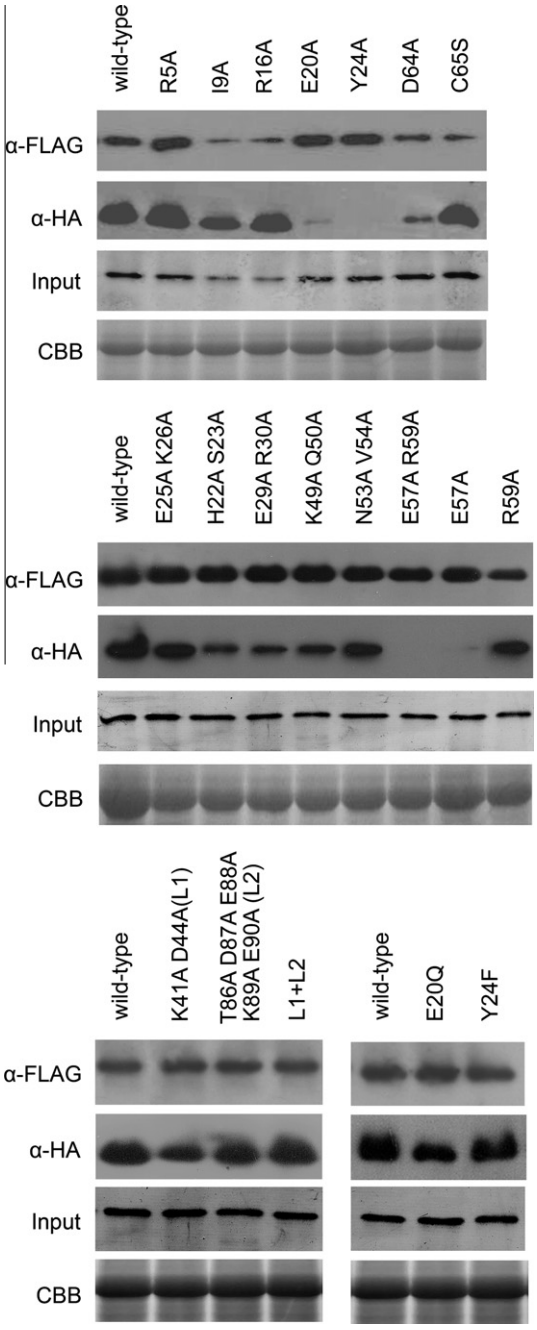

Fig. 3. Effects of KIS mutations on β-tubulin binding. Wild-type or mutants of KIS were coinfiltrated with FLAG-TUB9 into *N. benthamiana* leaves and coimmunoprecipitation assays were performed with anti-FLAG antibody. The immunoblot was performed as described in Fig. 2A. The input indicated the total soluble extracts that were subjected to immunoblotting with anti-HA antibody or stained with coomassie brilliant blue as loading control. The results shown are representative of four independent experiments.

Mutation of some helical residues, including Arg5, Ile9, Arg16, Asn53, Val54 and Arg59 showed no effect on binding, while some other helical mutants H22A S23A, E29A R30A and K49A Q50A are less effective in associating with β-tubulin (Fig. 3). In addition, decrease and increase on β-tubulin binding affinity were observed for D64A and C65S mutants, respectively, similar to the results of a previous study on human CoA [30]. To study the roles of loop region in the interaction, the L1 and L2 loops of KIS were mutated separately and simultaneously. Yet, none of the loop mutations had any effect on the interaction with β-tubulin (Fig. 3).

As a summary, the α-helical regions of KIS make contact with β-tubulin and residues Glu20, Tyr24 in the α1 helix, Glu57 in the α2 helix are key residues for β-tubulin recognition, whereas the loop regions are not crucial for this interaction.

4. Discussion

Microtubules play an essential role in a variety of cellular processes in plants. Microtubule function is considered to be dependent on microtubule associated proteins (MAPs) involved in microtubule dynamics and factors involved in microtubule biogenesis. Five TFCs (TFC A–E) have been functionally characterized in *Arabidopsis* [19,20,31–33]. In this study, we have determined the three-dimensional structure of *Arabidopsis* TFC A, which folds into a monomeric three-helix bundle in the same topology as Rbl2p monomer or human CoA, suggesting a conserved overall structure in the TFC A family. However, the oligomeric states of these three proteins are different. In the dimer structure of Rbl2p, there are 30 residues at the dimer interface and five of them (Ile8, Arg15, Glu19, Tyr23 and L65) have been confirmed to be important for the dimer formation through mutagenesis studies [18]. However, these residues except for Leu65 are rather conserved in human and *Arabidopsis*, which suggests there must be some other crucial residues responding to the assembly of monomers. It is suggested from sequences alignment that the hydrophobic residues at the Rbl2p dimer interface show lower sequence match especially for the residues Phe72, Leu65, Leu61 and Leu37 (Fig. 1C). Leu37 forms hydrophobic interaction with Ile8 from the other monomer, which is supposed to be important for dimerization. Leu61 forms hydrophobic interaction with the one from the other monomer, and also Leu65 altogether would form a hydrophobic core. Furthermore, the burying of Phe72 with large hydrophobic side chain would also enhance the hydrophobic dimer. While the corresponding four residues (Ala72, Cys65, Met61 and Met38) in KIS or (Ala74, Cys67, Met63 and Met40) in human CoA are either smaller or much less hydrophobic,

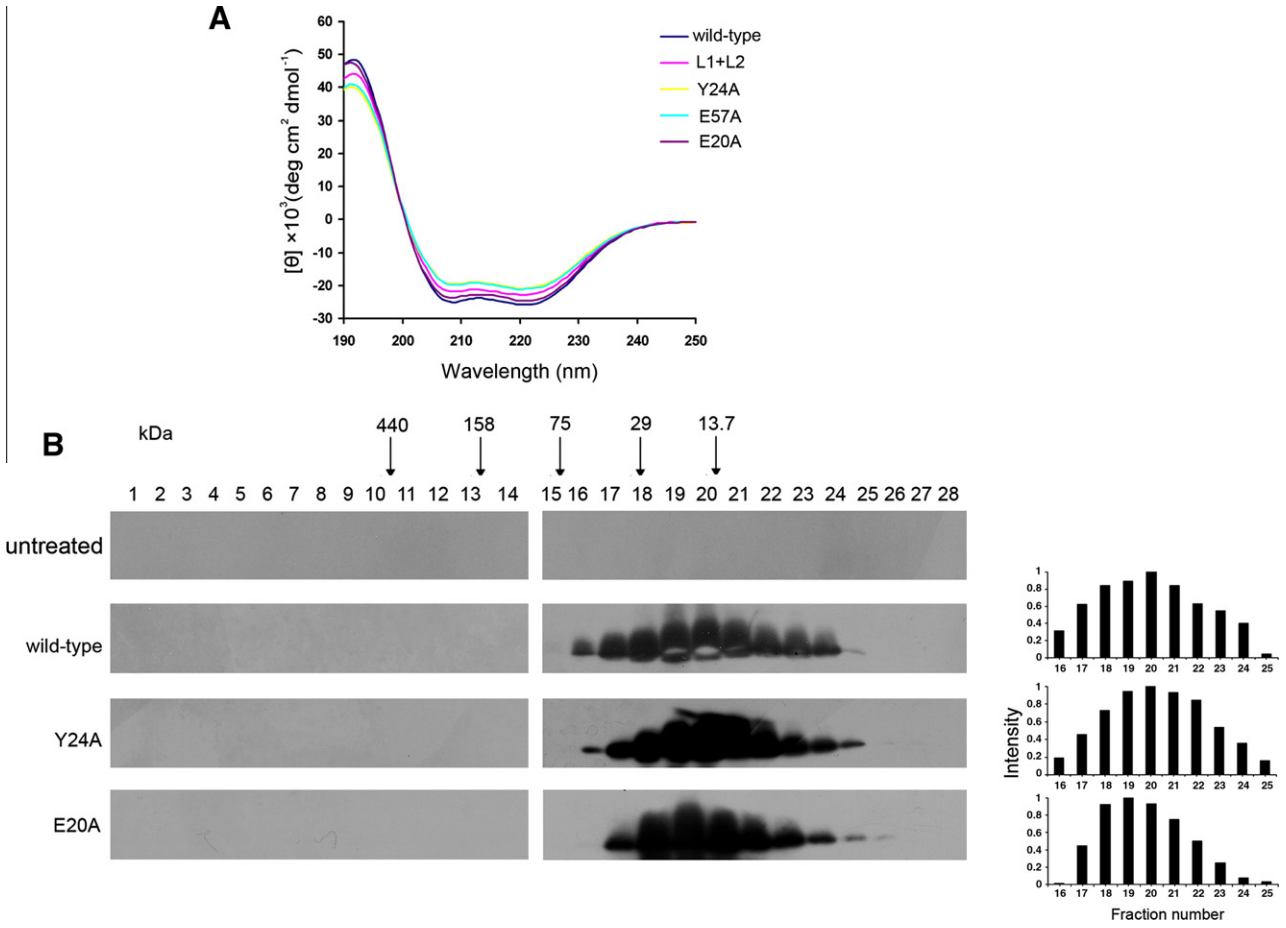

Fig. 4. (A) CD spectra of the WT and the mutant proteins. The different proteins are distinguished from each other by colors. (B) SEC analysis of protein extracts. Soluble protein from *N. benthamiana* leaves untreated or expressing wild-type or mutants of KIS were separated on Superdex 200 10/300 GL column. Fractions were collected and immunoblotted with anti-HA antibody. The elution volumes of molecular weight standards (kDa) are indicated. The histograms to the right of the immunoblots showed the relative intensity of the KIS bands. Chemiluminescence signals were quantified by densitometry and the strongest band in each blot was set to 1.

which may partially explain only monomer exists in human CoA and KIS. It is shown from the sequence comparison that these residues are rather conserved among most mammalians as well as plants, suggesting that the hydrophobic sequences appear to provide some insight into the monomer states of TFC A proteins in human and plants. Also more studies are needed to confirm the sequence specificity of the aggregation state of TFC A proteins in other organisms.

We demonstrated that KIS can also interact with β-tubulin in the plant cell and used site-directed mutagenesis to identify the residues of KIS that mediate β-tubulin binding. This method is limited by the caveat that single or double mutations may not be sufficient to disrupt protein–protein interaction. Still, we have found that three residues, Glu20, Tyr24 and Glu57, play an important role in β-tubulin binding and single mutation alone would abolish the β-tubulin recognition. Tyr24 is a highly conserved residue of the TFC A family with the exception of some species such as the *Schizosaccharomyces pombe* TFC A ($Alp31^A$), where the corresponding residue is Ala (Fig. 1C). Interesting, $Alp31^A$ can not associate with β-tubulin [34], which emphasizes the importance of Tyr24 in β-tubulin binding. Glu20 and Tyr24 are conserved and both Rbl2p mutagenesis studies and our work here on KIS have shown their crucial roles in β-tubulin recognition. However, they are quite different among different species at the molecular level. In Rbl2p, the corresponding residues Glu19 and Tyr23 are involved in dimerization through hydrogen-bonds as well as π–π interaction formed between two Tyr23. They are involved in β-tubulin binding through the maintenance of dimer status [18]. But in the monomer structures of KIS and human CoA, both Glu20 and Tyr24 are exposed to the solvent, and the aromatic ring of Tyr24 is nearly parallel to the axial helix of KIS as that of human CoA while the corresponding residue Tyr23 in Rbl2p is perpendicular to the axial helix (Fig. 5A and B). From the mutation analyses, we have shown that KIS binds to β-tubulin via the helical regions where Glu20 and Tyr24 located. Thus, this provides the hypothesis that the β-tubulin binding mechanism of KIS is more similar to that of human CoA rather than to Rbl2p.

Yeast, plant, and animal all have tubulin cofactors from A to E, and G-protein Arl2. This suggests that the pathway mediating the folding of tubulin may be evolutionarily conserved. Each of the TFC A orthologs in budding yeast, plant, and animal can interact with β-tubulin. However, *Rbl2p* is not an essential gene in yeast [14], while *KIS* and human CoA are important for cell viability [13,19,20]. It indicates that the mechanisms of TFC A-mediated β-tubulin folding and the importance of the folding for cell viability appear to be different between unicellular and multicellular organisms.

In summary, our structural and mutagenesis results presented here revealed features of β-tubulin binding to TFC A in plants. The α-helical residues of KIS are important for β-tubulin affinity. Further TFC A/β-tubulin complex structures will be necessary to understand the molecular mechanisms in atomic level in different organisms.

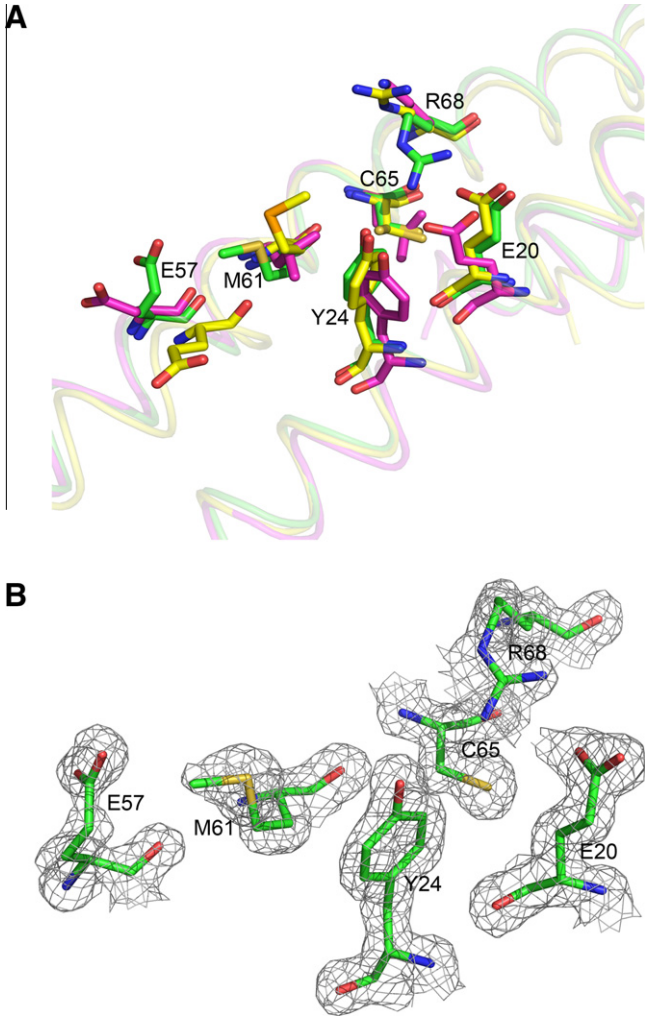

Fig. 5. (A) Superimposition of KIS (carbon atoms in green), human CoA (carbon atoms in yellow) and Rbl2p (carbon atoms in magenta) structures. Residues of KIS are labeled. (B) Stereoview of residue E20, E57, Y24 and the surrounding residues of Y24. The $2|F_o| - |F_c|$ omit map is represented at the 1.0σ level around the residues of interests.

Acknowledgements

We thank Dr. Kaituo Wang and Xiang Liu for invaluable advice. This work was supported by grants from the National Basic Research Program of China 973 (No. 2006CB101903 to W. C. H) and 985 and 211 from Peking University.

References

[1] Nogales, E., Whittaker, M., Milligan, R.A. and Downing, K.H. (1999) High-resolution model of the microtubule. Cell 96, 79–88.
[2] Lopez-Fanarraga, M., Avila, J., Guasch, A., Coll, M. and Zabala, J.C. (2001) Review: postchaperonin tubulin folding cofactors and their role in microtubule dynamics. J. Struct. Biol. 135, 219–229.
[3] Vainberg, I.E., Lewis, S.A., Rommelaere, H., Ampe, C., Vandekerckhove, J., Klein, H.L. and Cowan, N.J. (1998) Prefoldin, a chaperone that delivers unfolded proteins to cytosolic chaperonin. Cell 93, 863–873.
[4] Rommelaere, H., Van Troys, M., Gao, Y., Melki, R., Cowan, N.J., Vandekerckhove, J. and Ampe, C. (1993) Eukaryotic cytosolic chaperonin contains t-complex polypeptide 1 and seven related subunits. Proc. Natl. Acad. Sci. USA 90, 11975–11979.
[5] Tian, G., Lewis, S.A., Feierbach, B., Stearns, T., Rommelaere, H., Ampe, C. and Cowan, N.J. (1997) Tubulin subunits exist in an activated conformational state generated and maintained by protein cofactors. J. Cell Biol. 138, 821–832.
[6] Tian, G., Huang, Y., Rommelaere, H., Vandekerckhove, J., Ampe, C. and Cowan, N.J. (1996) Pathway leading to correctly folded β-tubulin. Cell 86, 287–296.
[7] Lewis, S.A., Tian, G. and Cowan, N.J. (1997) The α- and β-tubulin folding pathways. Trends Cell Biol. 7, 479–484.
[8] Fontalba, A., Paciucci, R., Avila, J. and Zabala, J.C. (1993) Incorporation of tubulin subunits into dimers requires GTP hydrolysis. J. Cell Sci. 106, 627–632.
[9] Bhamidipati, A., Lewis, S.A. and Cowan, N.J. (2000) ADP ribosylation factor-like protein 2 (Arl2) regulates the interaction of tubulin-folding cofactor D with native tubulin. J. Cell Biol. 149, 1087–1096.
[10] Campo, R., Fontalba, A., Sanchez, L.M. and Zabala, J.C. (1994) A 14 kDa release factor is involved in GTP-dependent β-tubulin folding. FEBS Lett. 353, 162–166.
[11] Gao, Y., Melki, R., Walden, P.D., Lewis, S.A., Ampe, C., Rommelaere, H., Vandekerckhove, J. and Cowan, N.J. (1994) A novel cochaperonin that modulates the ATPase activity of cytoplasmic chaperonin. J. Cell Biol. 125, 989–996.
[12] Fanarraga, M.L., Parraga, M., Aloria, K., del Mazo, J., Avila, J. and Zabala, J.C. (1999) Regulated expression of p14 (cofactor A) during spermatogenesis. Cell Motil. Cytoskeleton 43, 243–254.
[13] Nolasco, S., Bellido, J., Goncalves, J., Zabala, J.C. and Soares, H. (2005) Tubulin cofactor A gene silencing in mammalian cells induces changes in microtubule cytoskeleton, cell cycle arrest and cell death. FEBS Lett. 579, 3515–3524.
[14] Archer, J.E., Vega, L.R. and Solomon, F. (1995) Rbl2p, a yeast protein that binds to β-tubulin and participates in microtubule function in vivo. Cell 82, 425–434.
[15] Abruzzi, K.C., Smith, A., Chen, W. and Solomon, F. (2002) Protection from free β-tubulin by the β-tubulin binding protein Rbl2p. Mol. Cell Biol. 22, 138–147.
[16] Steinbacher, S. (1999) Crystal structure of the post-chaperonin β-tubulin binding cofactor Rbl2p. Nat. Struct. Biol. 6, 1029–1032.
[17] Guasch, A., Aloria, K., Perez, R., Avila, J., Zabala, J.C. and Coll, M. (2002) Three-dimensional structure of human tubulin chaperone cofactor A. J. Mol. Biol. 318, 1139–1149.
[18] You, L., Gillilan, R. and Huffaker, T.C. (2004) Model for the yeast cofactor A–β-tubulin complex based on computational docking and mutagenesis. J. Mol. Biol. 341, 1343–1354.
[19] Steinborn, K. et al. (2002) The *Arabidopsis PILZ* group genes encode tubulin-folding cofactor orthologs required for cell division but not cell growth. Genes Dev. 16, 959–971.
[20] Kirik, V. et al. (2002) The *Arabidopsis* tubulin-folding cofactor A gene is involved in the control of the α/β-tubulin monomer balance. Plant Cell 14, 2265–2276.
[21] Gu, Y., Deng, Z., Paredez, A.R., DeBolt, S., Wang, Z.Y. and Somerville, C. (2008) Prefoldin 6 is required for normal microtubule dynamics and organization in *Arabidopsis*. Proc. Natl. Acad. Sci. USA 105, 18064–18069.
[22] Lu, L., Nan, J., Mi, W., Wei, C., Li, N. and Li, Y. (2010) Crystallization and preliminary X-ray analysis of tubulin folding cofactor A from *Arabidopsis thaliana*. Acta Crystallogr., Sect. F, in press, doi:10.1107/S1744309110023900.
[23] Vagin, A.T.A. (1997) MOLREP: an automated program for molecular replacement. J. Appl. Crystallogr. 30, 1022–1025.
[24] Adams, P.D. et al. (2002) PHENIX: building new software for automated crystallographic structure determination. Acta Crystallogr., Sect. D 58, 1948–1954.
[25] Emsley, P. and Cowtan, K. (2004) Coot: model-building tools for molecular graphics. Acta Crystallogr., Sect. D 60, 2126–2132.
[26] Laskowski, R.A., MAcArthur, M.W., Moss, D.S. and Thornton, J.M. (1993) PROCHECK: a program to check the stereochemical quality of protein structures. J. Appl. Crystallogr. 26, 283–291.
[27] Restrepo, M.A., Freed, D.D. and Carrington, J.C. (1990) Nuclear transport of plant potyviral proteins. Plant Cell 2, 987–998.
[28] Walter, M. et al. (2004) Visualization of protein interactions in living plant cells using bimolecular fluorescence complementation. Plant J. 40, 428–438.
[29] Tai, T.H., Dahlbeck, D., Clark, E.T., Gajiwala, P., Pasion, R., Whalen, M.C., Stall, R.E. and Staskawicz, B.J. (1999) Expression of the Bs2 pepper gene confers resistance to bacterial spot disease in tomato. Proc. Natl. Acad. Sci. USA 96, 14153–14158.
[30] Llosa, M., Aloria, K., Campo, R., Padilla, R., Avila, J., Sanchez-Pulido, L. and Zabala, J.C. (1996) The β-tubulin monomer release factor (p14) has homology with a region of the DnaJ protein. FEBS Lett. 397, 283–289.
[31] Kirik, V. et al. (2002) Functional analysis of the tubulin-folding cofactor C in *Arabidopsis thaliana*. Curr. Biol. 12, 1519–1523.
[32] Dhonukshe, P., Bargmann, B.O. and Gadella Jr., T.W. (2006) *Arabidopsis* tubulin folding cofactor B interacts with α-tubulin in vivo. Plant Cell Physiol. 47, 1406–1411.
[33] Du, Y., Cui, M., Qian, D., Zhu, L., Wei, C., Yuan, M., Zhang, Z. and Li, Y. (2010) *AtTFC B* is involved in control of cell division. Front. Biosci. J. 1, 752–763.
[34] Radcliffe, P.A., Garcia, M.A. and Toda, T. (2000) The cofactor-dependent pathways for α- and β-tubulins in microtubule biogenesis are functionally different in fission yeast. Genetics 156, 93–103.
[35] Thompson, J.D., Higgins, D.G. and Gibson, T.J. (1994) CLUSTAL W: improving the sensitivity of progressive multiple sequence alignment through sequence weighting, position-specific gap penalties and weight matrix choice. Nucleic Acids Res. 22, 4673–4680.
[36] Gouet, P., Courcelle, E., Stuart, D.I. and Metoz, F. (1999) ESPript: analysis of multiple sequence alignments in PostScript. Bioinformatics 15, 305–308.